Supporting Information

Synergistic electrolyte engineering with TEABH4 additive: achieving oriented deposition and ultralong cycling in magnesium metal batteries†

Qi Sun[a, b, c], Shaohua Luo[a, b, c*], Wei Zhao [a, b, c], Xin Yan [a, b, c], Rui Huang [a, b, c], Yicheng Lin [a, b, c], Qiuyue Liu[a, b, c], Shengxue Yan[a, b, c], Xiaoping Lin[a, b, c]

a. School of Materials Science and Engineering, Northeastern University, Shenyang 110819, P. R. China

b. School of Resources and Materials, Northeastern University at Qinhuangdao, Qinhuangdao 066004, P. R. China

c. Hebei Key Laboratory of Dielectric and Electrolyte Functional Material, Qinhuangdao 066004, P. R. China

**Corresponding author: tianyanglsh@163.com (S. H. Luo)*

List of medicines:

Magnesium trifluoromethanesulfonate ($Mg(CF_3SO_3)_2$, 98.0%, Aladdin), Aluminium chloride ($AlCl_3$, 99.0%, Aladdin), Diethylene glycol dimethyl ether (G2, ≥98% contains 50-150 ppm BHTas stabilizer, Aladdin), Tetraethylammonium borohydride ($TEABH_4$, 98.0%, Aladdin), Molybdenum disulfide (MoS_2, 98.0%, Aladdin), Copper (Cu, 99.9%, Aladdin), Molybdenum powder (Mo, 99.9%, Aladdin), Iodine (I_2, 99.8%, Aladdin), Super P (Canrd Technology Co. Ltd.), Polyvinylidene Fluoride (PVDF, Canrd Technology Co. Ltd.), and 1-Methyl-2-pyrrolidinone(NMP, 99.0%, Aladdin).

The preparation of electrolytes

Preparation of MA-G2 Electrolyte:

A 0.2 M solution of $Mg(CF_3SO_3)_2$ was prepared by dissolving the salt in 2 mL of G2 solvent under an argon atmosphere, followed by magnetic stirring for at least 8 hours. Subsequently, $AlCl_3$ was gradually added to the 0.2 M $Mg(CF_3SO_3)_2$/G2 solution at a 1:1 molar ratio under continuous stirring. Prior to electrochemical applications, the resulting mixture was vigorously stirred at room temperature for an additional 8 hours to ensure homogeneity, yielding the MA-G2 electrolyte.

Preparation of MAT-G2 Electrolyte:

The MA-G2 electrolyte was further modified via gradual addition of $TEABH_4$ at controlled stoichiometric ratios ($Mg(CF_3SO_3)_2$:$AlCl_3$:$TEABH_4$ = 2:2:0.5, 2:2:1, 2:2:2, 2:2:3). Each formulation underwent 8 h of continuous stirring under moisture-free conditions to achieve homogeneity.

The preparation of cathode:

Mo_6S_8 powders were synthesized stepwise according to previous reportsMo_6S_8[1]. The Mo_6S_8 cathode was made by blending Mo_6S_8 power, Super P, and PVDF with a weight ratio of 8: 1: 1 to form the slurry, and then coated on the Ni foil. After drying at 60 °C under vacuum overnight, the loading mass of obtained electrodes was controlled to be ~ 1.2 mg cm^{-2}.

Materials characterization

The Karl Fischer moisture titrator (Metrohm 831) was used to check the moisture content of the electrolyte. The morphologies of the two electrodes were observed by scanning electron microscope (SEM, Regulus8100) and energy-dispersive spectrometry (EDS, 80 mm2 X-MaxN Silicon Drift Detector). The X-ray diffraction (XRD, Rigaku Smartlab) and X-ray photoelectron spectroscopy (Thermo Scientific K-Alpha) were used to detect the composition of the electrode. FTIR-8400S was used for Fourier translation infrared spectroscopy (FT-IR) examination. Raman spectra were obtained using a Renishaw INVIA micro-Raman spectroscopy system. NMR spectra were obtained using Bruker 600MHz instrument. X-ray photoelectron spectroscopy (XPS) measurements were carried out using Thermo Scientific K-Alpha XPS instrument.

The electrochemical tests

All battery (2032 type battery) assemblies were carried out in a glove phase filled with argon, with water and oxygen content less than 0.1 ppm. The symmetric cells were assembled using two pristine Mg anodes, a glass fiber (Whatman TM GF/D) and electrolyte (120 μL for each cell). The polarization curve, electrochemical impedance spectroscopy (EIS) and direct current-voltage measurement were performed on a CS350M electrochemical workstation. The frequency of EIS is between 100 kHz and 0.1 Hz with a sinusoidal voltage of 5 mV amplitude. The cycle stability of the anode was also tested by assembling Mg||Mg symmetrical batteries. The coulombic efficiency (CE) of the batteries was tested by assembling the Mg||Cu asymmetric batteries. For the Mg||Mo_6S_8 full batteries with two different prepared electrodes, and the voltage range was 0.2-1.8 V. Different current densities were applied to test its cycle stability and rate capacities.

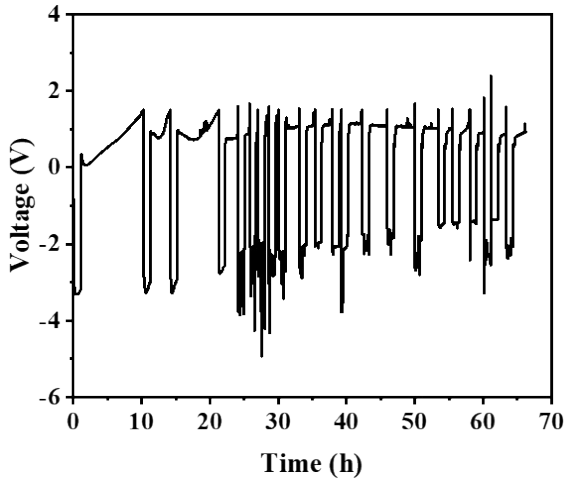

Fig. S1. The discharge-charge curves of Mg||Cu asymmetric cell with the electrolytes of 0.2 M $Mg(CF_3SO_3)_2$ in G2.

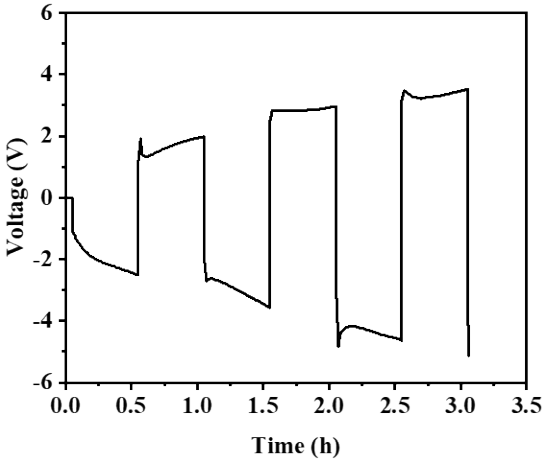

Fig. S2. The discharge-charge curves of Mg||Mg symmetric cell with the electrolytes of 0.2 M $Mg(CF_3SO_3)_2$ in G2.

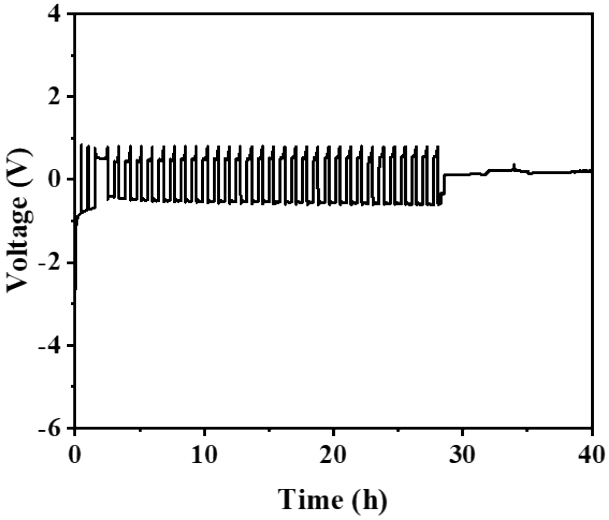

Fig. S3. The discharge-charge curves of Mg||Cu asymmetric cell with the electrolytes of 0.2 M $Mg(CF_3SO_3)_2$ in G2.

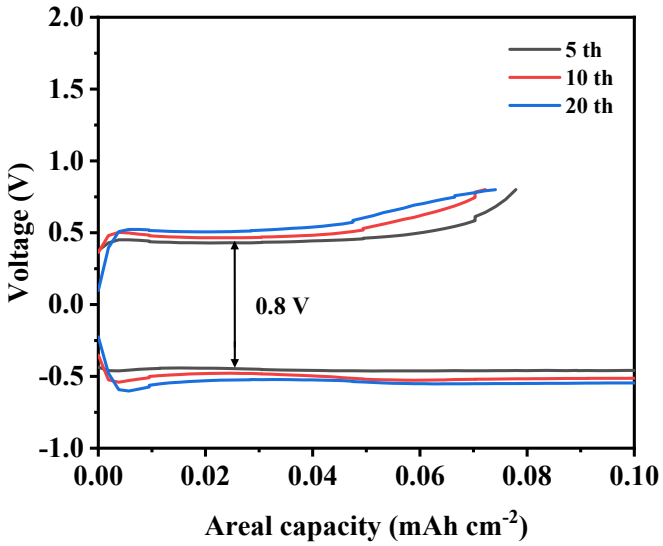

Fig. S4. Voltage profiles of Mg||Cu asymmetric cell at an areal capacity of 0.1 mAh cm^{-2} and current density of 0.1 mA cm^{-2}.

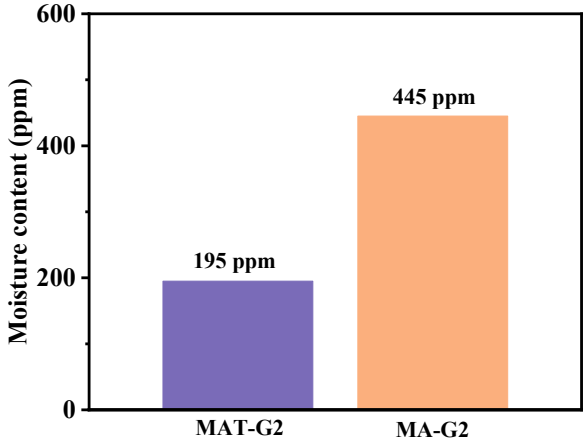

Fig. S5. Moisture content of MAT-G2 and MA-G2 electrolytes determined with Karl Fischer moisture titrator.

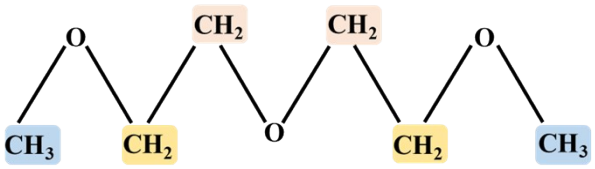

Fig. S6. Structural formula of diethylene glycol dimethyl ether.

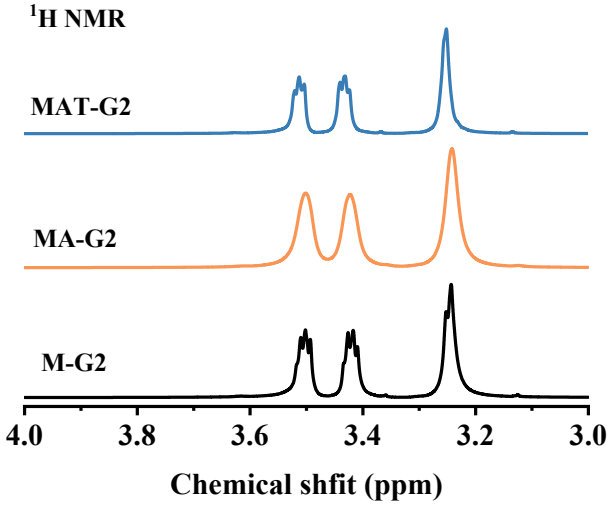

Fig. S7. ^{1}H NMR spectra of MA-G2 and MAT-G2 electrolytes compared to 0.2 M $Mg(CF_3SO_3)_2$ in G2.

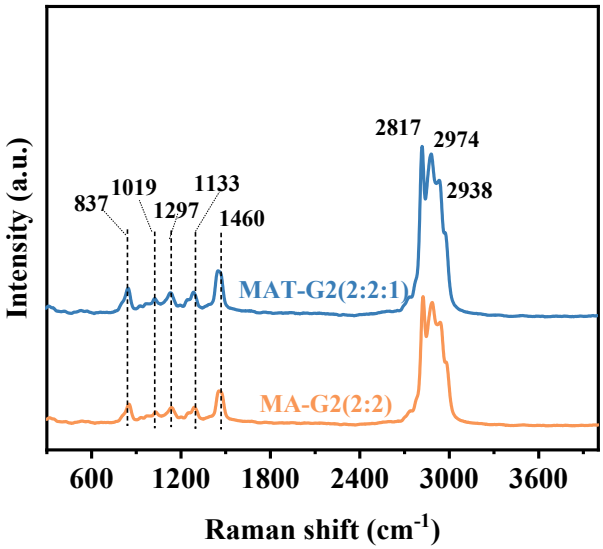

Fig. S8. Raman profiles of MA-G2 and MAT-G2 electrolytes.

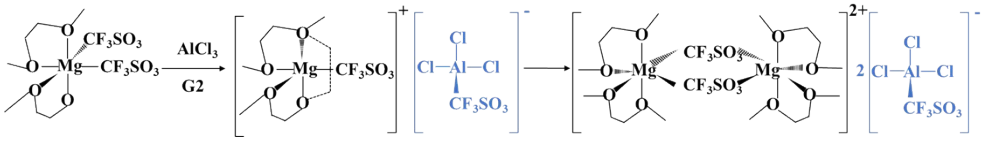

Fig. S9. Possible reaction pathway schemes for the MAT-G2 electrolyte.

Table S1. Electrochemical data of Mg||Cu cells with different modified electrolytes.

Electrolyte	Current Density (mA cm^{-2})	Areal Capacity (mAh cm^{-2})	Cycle Numbers	Coulombic Efficiency
MAT (2:2:0.5)	0.1	0.1	900	88.84
MAT (2:2:1)	0.1	0.1	1500	97.2
MAT (2:2:2)	0.1	0.1	2000	97.3
MAT (2:2:3)	0.1	0.1	800	91.6

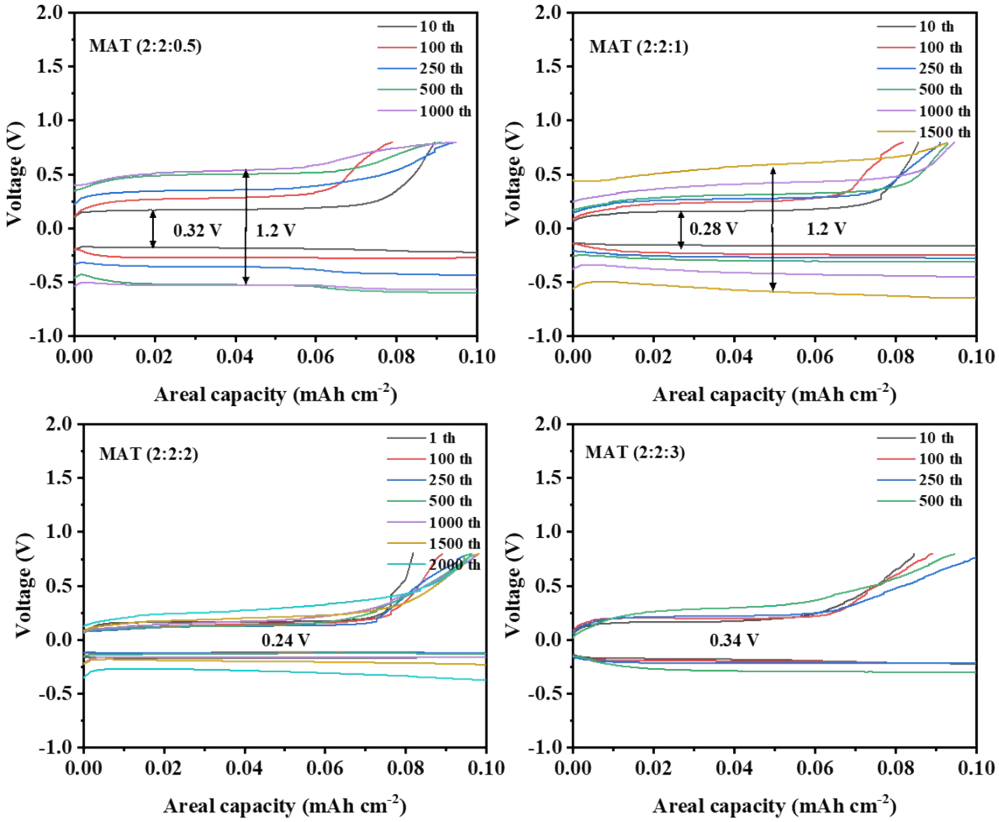

Fig. S10. Voltage profiles of Mg||Cu asymmetric cell at an areal capacity of 0.1 mAh cm^{-2} and current density of 0.1 mA cm^{-2}.

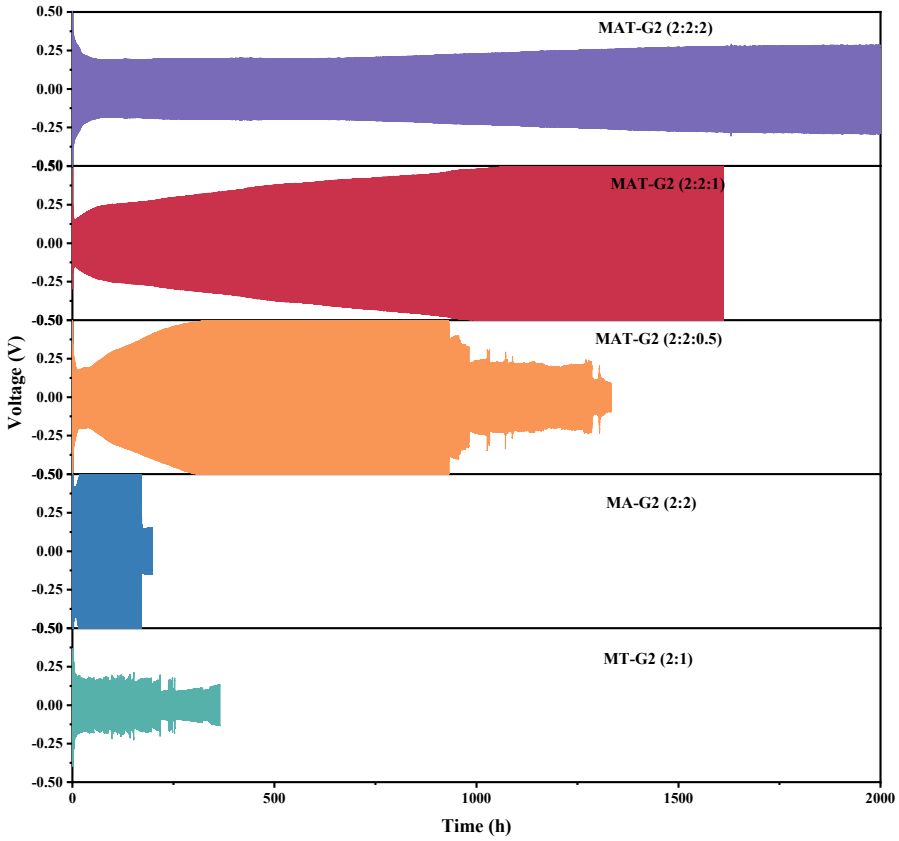

Fig. S11. Cycling curves of Mg||Mg symmetric cells.

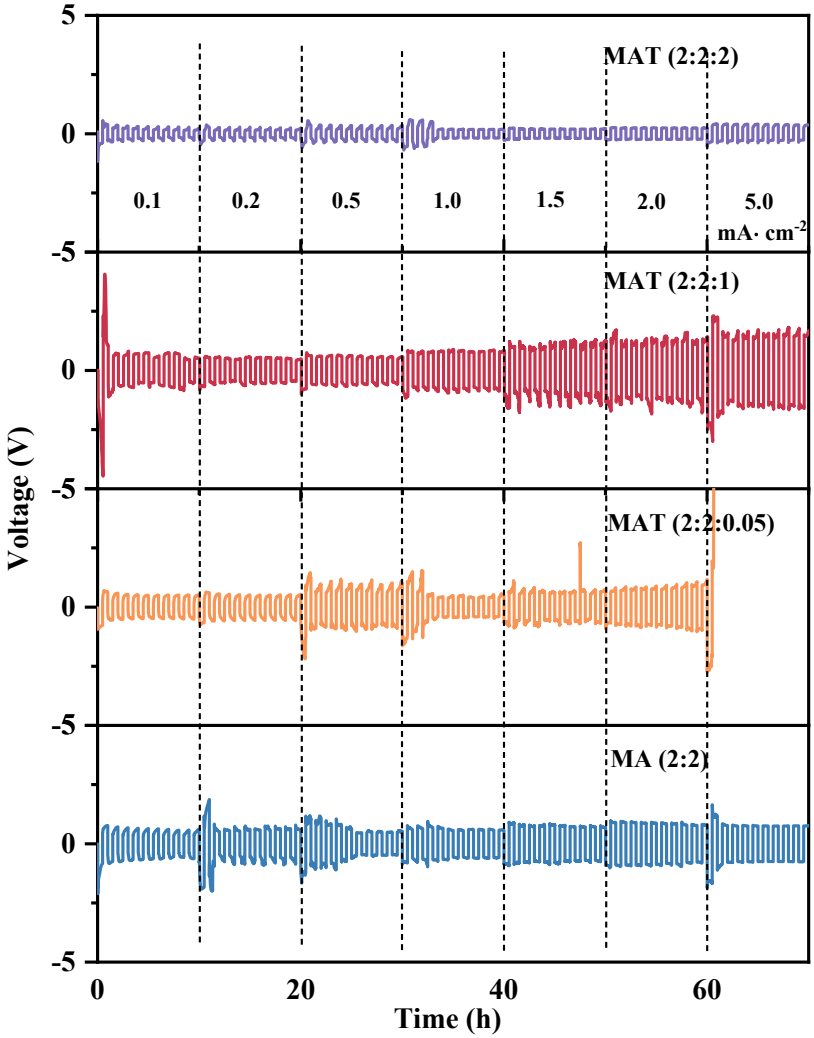

Fig. S12. Multiplicity performance of Mg||Mg symmetric cells with different electrolytes at different current densities.

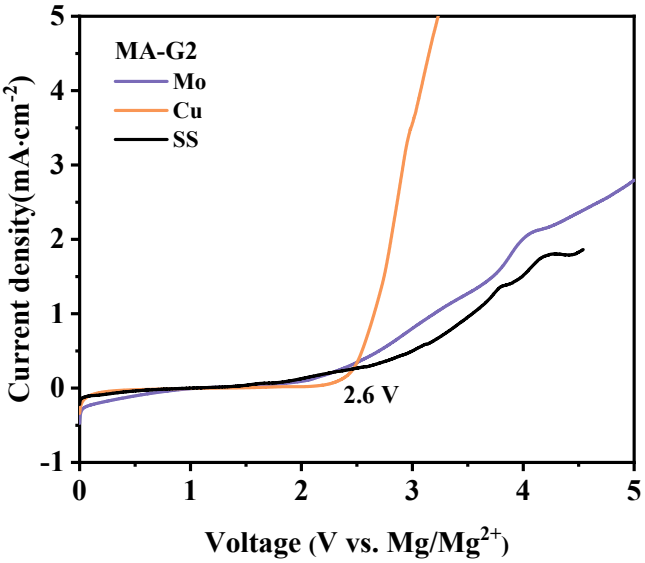

Fig. S13. LSV curves of the MA-G2 electrolytes on Cu, Mo and SS electrode.

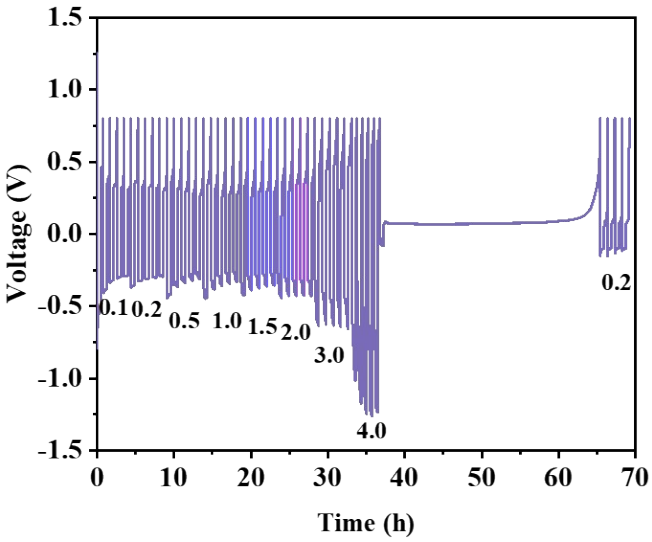

Fig. S14. Multiplication performance of MAT electrolyte Mg||Cu asymmetric cells at different current densities.

Table S2. Performance comparison of the reported Mg||Mg cells in different Mg electrolytes.

Electrolytes	**current density (mA cm^{-2})**	**Areal capacity (mAh cm^{-2})**	**Overpotential (mV)**	**Cycling number**	**Reference**
$Mg(CF_3SO_3)_2$ +$MgCl_2$ in DME	0.50	1.00	220	125	[2]
$Mg(CF_3SO_3)_2$ +TBAC in DME	0.50	0.50	250	600	[3]
MTD-MOEA (1:8)	0.50	0.25	100	5000	[4]
$Mg(CF_3SO_3)_2$ /DME/G2/MOEA	0.10	0.05	150	1000	[5]
$Mg(CF_3SO_3)_2$ +$AlCl_3$+$MgCl_2$ in DME	0.05	0.25	250	200	[6]
MAT-G2	0.10 1.00	0.05 0.50	250 400	2000 3500	This work

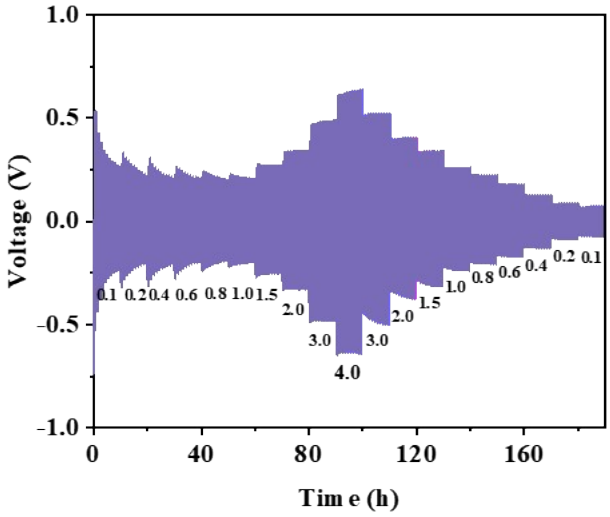

Fig. S15. Multiplicity performance test of MAT-G2 electrolyte.

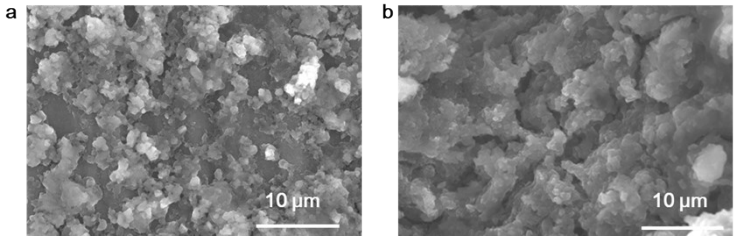

Fig. S16. SEM diagram of Mg anodes in (a) MAT-G2 and (b) MA-G2 electrolytes at current densities of 2 mA cm^{-2}.

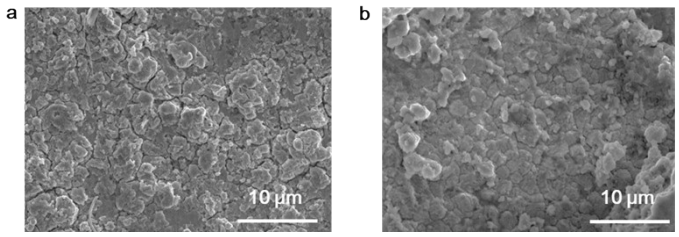

Fig. S17. SEM images of Mg deposited on Cu foil in (a) MAT-G2 and (b) MA-G2 electrolytes.

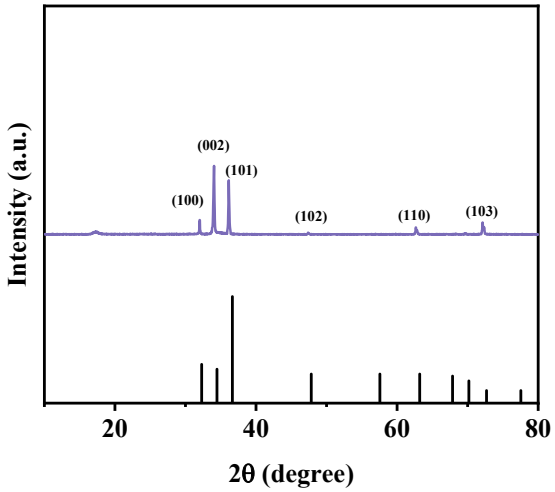

Fig. S18. XRD of cycle number and average CE of the Mg||Cu cells in this work at 0.5 mA cm^{-2} with those in literature.

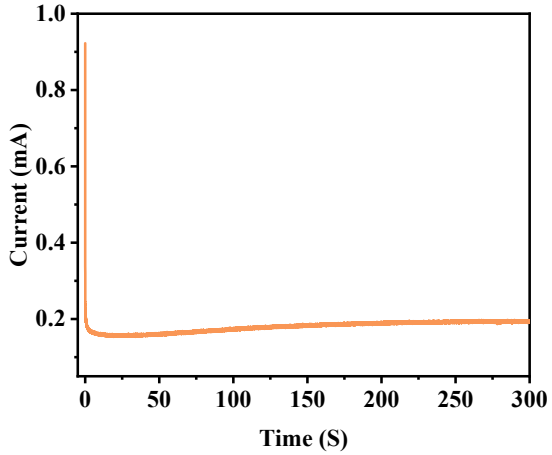

Fig. S19. The chronoamperometric current tests are carried out on Mg|MAT-G2|Mg symmetric cells.

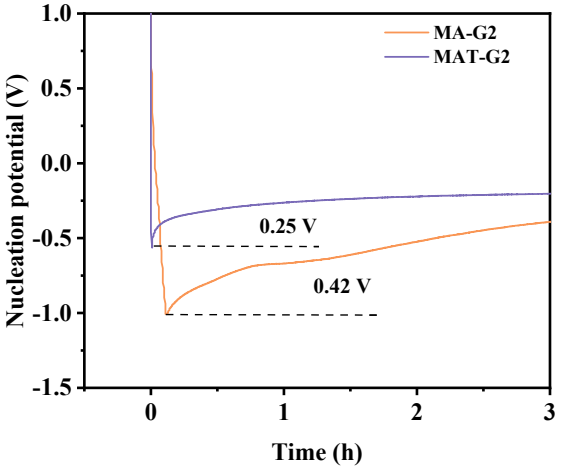

Fig. S20. Comparison of deposition profiles of Mg|MAT-G2|Cu and Mg|MA-G2|Cu asymmetric cells.

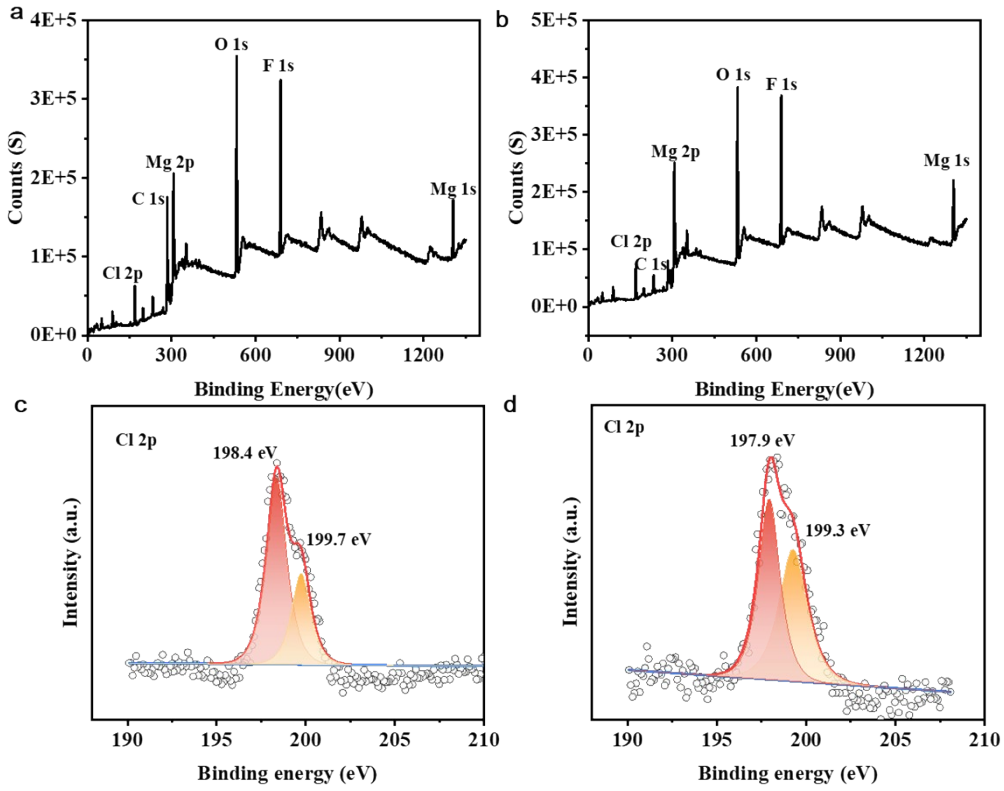

Fig. S21. XPS analysis of the magnesium anode after cycling in (a, c) MA and (b, d) MAT electrolytes.

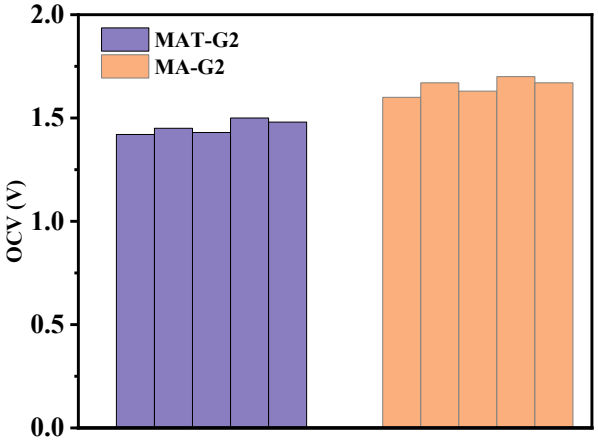

Fig. S22. The open-circuit voltage (OCV) of Mg||Mo_6S_8 full cells with different electrolytes.

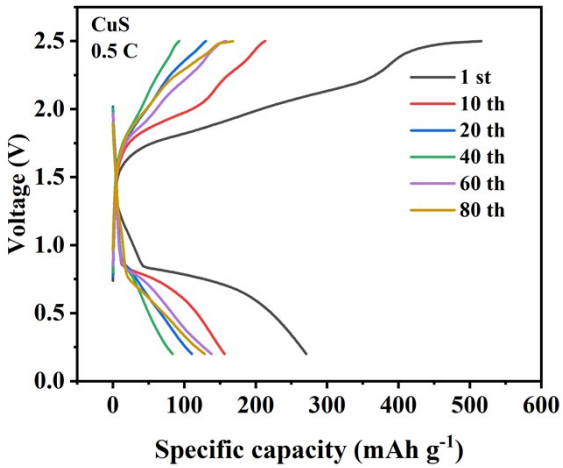

Fig. S23. Mg|MAT-G2|CuS full cell performance in MAT-G2 electrolyte at 0.5 C.

References

1. M. Mao, Z. Lin, Y. Tong, J. Yue, C. Zhao, J. Lu, Q. Zhang, L. Gu, L. Suo, Y.-S. Hu, H. Li, X. Huang and L. Chen, Iodine Vapor Transport-Triggered Preferential Growth of Chevrel Mo6S8 Nanosheets for Advanced Multivalent Batteries, *ACS Nano*, 2020, **14**, 1102-1110.
2. D.-T. Nguyen, A. Y. S. Eng, M.-F. Ng, V. Kumar, Z. Sofer, A. D. Handoko, G. S. Subramanian and Z. W. Seh, A High-Performance Magnesium Triflate-based Electrolyte for Rechargeable Magnesium Batteries, *Cell Reports Physical Science*, 2020, **1**, 100265.
3. D.-T. Nguyen, A. Y. S. Eng, R. Horia, Z. Sofer, A. D. Handoko, M.-F. Ng and Z. W. Seh, Rechargeable magnesium batteries enabled by conventional electrolytes with multifunctional organic chloride additives, *Energy Stor. Mater.*, 2022, **45**, 1120-1132.
4. D. Zhang, Y. Wang, Y. Yang, Y. Zhang, Y. Zhao, M. Pan, Y. Sun, S. Chen, X. Liu and J. Wang, Constructing Efficient $Mg(CF_3SO_3)_2$ Electrolyte via Tailoring Solvation and Interface Chemistry for High-Performance Rechargeable Magnesium Batteries, *Adv. Energy Mater.*, 2023, **13**, 2301795.
5. Y. Du, Y. Chen, S. Tan, J. Chen, X. Huang, L. Cui, J. Long, Z. Wang, X. Yao, B. Shang, G. Huang, X. Zhou, L. Li, J. Wang and F. Pan, Strong solvent coordination effect inducing gradient solid-electrolyte-interphase formation for highly efficient Mg plating/stripping, *Energy Stor. Mater.*, 2023, **62**, 102939.
6. D. Huang, S. Tan, M. Li, D. Wang, C. Han, Q. An and L. Mai, Highly efficient non-nucleophilic $Mg(CF_3SO_3)_2$-based electrolyte for high-power Mg/S battery, *ACS Appl. Mater. Interfaces*, 2020, **12**, 17474-17480.